Gümüşhane University Journal of Science

GUFBD / *GUJS* (2023) 13(4): 1073-1081 doi: 10.17714/gumusfenbil.1317131 Research Article

Detection of buried objects with different material properties by ground penetrating radar (GPR) method

Farklı malzeme özelliklerine sahip gömülü nesnelerin yer radarı (GPR) yöntemiyle tespit edilmesi

Mahmut SARI *[1]

[1]*Gümüşhane University, Gümüshane Vocational School, Construction Department, 29100, Gümüşhane*

• Received: 20.06.2023 • Accepted: 15.09.2023

Abstract

GPR, which permits the capture of high-resolution subterranean data, has developed into a key geophysical technique for determining the depth, geometry, boundaries, and volumes of buried shallow objects. In this study, the detectability of the location, size, and physical property parameters of buried objects with the ground radar method was revealed by creating a laboratory environment in real field conditions. For this purpose, a realistic laboratory environment with a depth and length of 5 m was created on the filled soil material at the test site, and buried objects with different material properties were placed. In addition, by adding sand material to the middle part of the soil fill material in the test area, its situation in different layers was tried to be examined. GPR data were collected on the models using the RAMAC CU II system and a 500 MHz center frequency shield antenna. After processing the data, reflected/scattered electromagnetic (EM) wave fields on the radargram of a profile perpendicular to the buried objects were examined. In this way, the positions, sizes, physical properties (types) of buried objects along with their depths and their situations in different layer environments have been revealed. According to the results, the peak width of hyperbolas and the sizes of buried objects were determined on the processed radargrams. The types of buried objects and their situations in different layer environments are clearly revealed. The scattered wave field amplitudes of the plastic pipe (A and C regions) from the reflection coefficients are substantially lower than the scattered wave field amplitudes of the iron pipe (B region) from the buried objects. It is thought that the strong reflections extending from the C region to the deep on the radar are caused by the lead blocks in the plastic pipe.

Keywords: Buried objects, Ground penetrating radar, Shallow geophysics

Öz

Yüksek çözünürlüklü yeraltı verisi alınmasına olanak sağlayan GPR, gömülü sığ nesnelerin derinlik, geometri, sınır ve hacimlerinin hesaplanmasında önemli bir jeofizik yöntem haline gelmiştir. Bu çalışmada, yer radarı yöntemi ile gömülü nesnelerin konum, büyüklük ve fiziksel özellik parametrelerinin tespit edilebilirliği, gerçek arazi şartlarında laboratuvar ortamı oluşturularak ortaya konulmuştur. Bu amaçla, test sahasında dolgu toprak malzeme üzerinde derinlik ve uzunluğu 5 m olacak şekilde gerçeğe yakın bir laboratuvar ortamı oluşturulup farklı malzeme özelliklerinde gömülü nesneler yerleştirilmiştir. Ayrıca, test sahasındaki toprak dolgu malzemenin orta kısmına kum malzeme eklenerek farklı tabakalardaki durumu da irdelenmeye çalışılmıştır. GPR verileri, modeller üzerinde RAMAC CU II sistem ve 500 MHz merkez frekanslı kapalı anten kullanılarak toplanmıştır. Veriler işlendikten sonra gömülü nesnelere dik bir profile ait radargram üzerinde yansımış/ saçılmış elektromanyetik (EM) dalga alanları irdelenmiştir. Böylece gömülü nesnelerin derinlikleri ile birlikte konumları, büyüklükleri, fiziksel özellikleri (cinsleri) ve farklı tabaka ortamlarındaki durumları ortaya konulmuştur. Sonuçlara göre, işlenmiş radargramlar üzerinde hiperbollerin tepe genişliği gömülü nesnelerin büyüklükleri belirlenmiştir. Gömülü nesnelerin cinsleri ve farklı tabaka ortamlarındaki durumları net bir şekilde ortaya koyulmuştur. Plastik borunun yansıma katsayılarından saçılan dalga alanı genlikleri (A ve C bölgeleri), gömülü nesnelerden demir borudan saçılan dalga alanı genliklerinden (B bölgesi) önemli ölçüde düşük olduğu görülmüş. Radargam üzerinde C bölgesinden derine doğru uzanan kuvvetli yansımaların sebebinin plastik boru içerisindeki kurşun bloklardan kaynaklandığı düşünülmektedir.

***Anahtar kelimeler**: Gömülü nesneler, Yer radarı, Sığ jeofizik*

* Mahmut SARI; msari@gumushane.edu.tr

1. Introduction

Ground Penetrating Radar (GPR) is one of the important methods used to investigate the physical properties of structures in near-surface environments and the environments surrounding these structures. The position of the centimeter-sized target structures and their buried depths can be found with the use of suitable antenna selections in environments where ground radar measurements are feasible, such as those without substantial clay and water content. GPR is used in geotechnical applications to determine the underground properties of the areas where engineering structures will be built and to examine the reinforcements of these structures (Hugenschmidt, 2002; Sari & Öztürk, 2018; Sariçiçek & Şeren, 2020), in archaeological studies (Aydın et al., 2022; Neubauer et al., 2002) determination of buried structures and environments that cause environmental problems (Carcione et al., 2003; Kurt et al., 2009; Kurtulmuş & Drahor, 2008; Uyar, 2017), revealing and mapping infrastructure features and problems in urban areas (Zeng & McMechan, 1997), revealing the sedimentary layer stacking features and lake floors and water depths in river and lake areas (Streich et al., 2006) in forensic research (Hammon III et al., 2000), identification of landmines (Lopera et al., 2007) and determination of ice thickness (Annan & Davis, 1977). It has become one of the most widely used methods of shallow geophysical research today, as it gives successful results in similar special subjects.

In this study, GPR measurements were taken in the garden of Gümüshane University Vocational School of Health Sciences by choosing the filled soil area (shown in red rectangle) as the test site (Figure 1). The detectability of the location, size, and physical characteristics of buried objects with the ground radar method in the test area was demonstrated by creating a laboratory environment in real field conditions. After processing the GPR data, the reflected/scattered electromagnetic (EM) wave fields on the radargram of a profile perpendicular to the buried objects were examined, and their positions, sizes, physical properties (types) and status in different layer environments were determined along with the depth of the buried objects. Without prior information of the locations, sizes, or types of pipes, this investigation will reveal changes in depth as well as the types and sizes of subterranean pipes.

Figure1. Location map of study area

2. Material and method

GPR is an electromagnetic technique that can produce high-resolution images of the area being studied at shallow depths (Davis & Annan, 1986). GPR method encounters discontinuities with different dielectric properties and buried objects (pipes, foundation, etc.) during the propagation of high center frequency electromagnetic radar signals sent underground. In this case, it is based on the principle of reflecting some of the energy back and recording the double path travel time of the wave in nanoseconds with the receiving antennas on the surface (Figure 2a). Three alternative kinds of picture data can be produced during GPR scans. These GPR images are referred to as A-, B-, and C-scan images. Time-dependent data from a single spot on the surface make up the A-scan signals (Figure 2b). The A-scan signals from the following places are combined to create the B-scan image (Figure 2c).

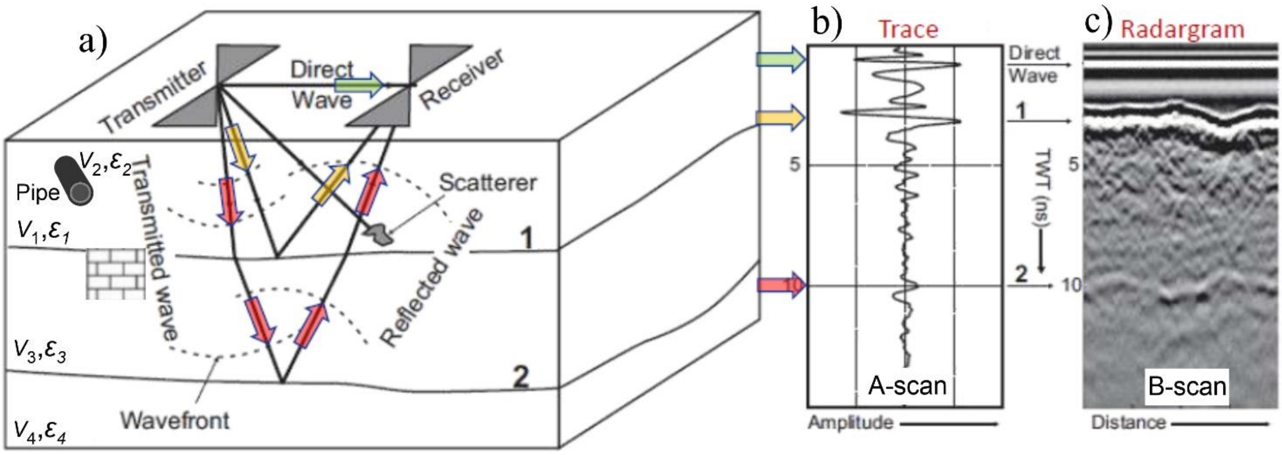

Figure 2. a) Working principle of GPR method b) GPR A-scan image, c) GPR B-scan image (ULiege & BGS, n.d)

The separation between these interfaces must be at least one wavelength of the radar energy traveling between them in order to detect reflections from two different parallel planes of a buried structure (Davis & Annan, 1989). If these two interfaces are closer to each other than the radar wavelength, they will either disappear or go unnoticed due to the interference of reflections from the upper and lower surfaces. In the opposite case, two separate reflections are obtained from these two interfaces and the sought structure can be determined. The reflection waves from a single mapped buried surface can be observed regardless of the radar wavelength that penetrates the surroundings if this surface creates a reflection that cannot be confused with other nearby structures. However, if this surface is an irregular or undulating surface, higher subsurface resolution is required to image it correctly. GPR signals can reach depths of approximately 50-60 m in materials or environments with low conductivity such as dry sand, granite or marble (Table 1). Wet clay, shale and other highly conductive materials absorb GPR signals, thus limiting the depth (penetration depth) that this signal can reach to 1 m or less. High-frequency antennas increase the resolution while the depth of search decreases (Daniels, 2004; Davis & Annan, 1989). In this study, information was obtained from a depth of approximately 5m using the RAMAC CU II system 500 MHz center frequency indoor antenna.

Table 1. Approximate depth ranges for different antenna frequencies (Ramac/GPR, n.d).

Antenna Frequency (MHz)	Lower limit of object target size (m)	Approximate depth range * (m)	Approximate penetration Depth (m)
100	0.1-1	2-15	15-25
250	0.05-0.5	1-10	5-15
500	**0.04**	**1-5**	**3-10**
800	0.02	0.4-2	1-6

*In normal geological environment absent of low resistive layers

The most effective method used to determine the types of pipes is to investigate the amplitude size and polarity. The reflection coefficient of the reflected or dispersed wave from the pipe provides the simplest explanation for why the polarity is the same or different as well as the amplitude information. The reflection coefficient is for the wave perpendicular to the pipe;

$$R = \frac{V_2 - V_1}{V_2 + V_1} = \frac{\sqrt{\varepsilon_1} - \sqrt{\varepsilon_2}}{\sqrt{\varepsilon_1} + \sqrt{\varepsilon_2}} \quad (1)$$

is defined by the relation (Annan, 2005). Here, V_1 and $\mathcal{E}_1$ are respectively; It shows the EM wave velocity and dielectric coefficient of the environment (dry sand poured into the work area) in which the pipe is located. V_2 and $\mathcal{E}_2$ are respectively; represents the EM wave velocity and dielectric coefficient of the pipes.

3. Data acquisition: GPR mapping and surveying

In the garden of Gümüşhane University Vocational School of Health Sciences, A and C: Plastic pipes (40 cm in diameter, 47 cm in length, sewage waste pipe), with different material properties to be buried in the fill soil test site, B: Iron fuel tank (30 cm in diameter, 68 cm in length, truck fuel tank) and lead blocks selected (Figure 3).

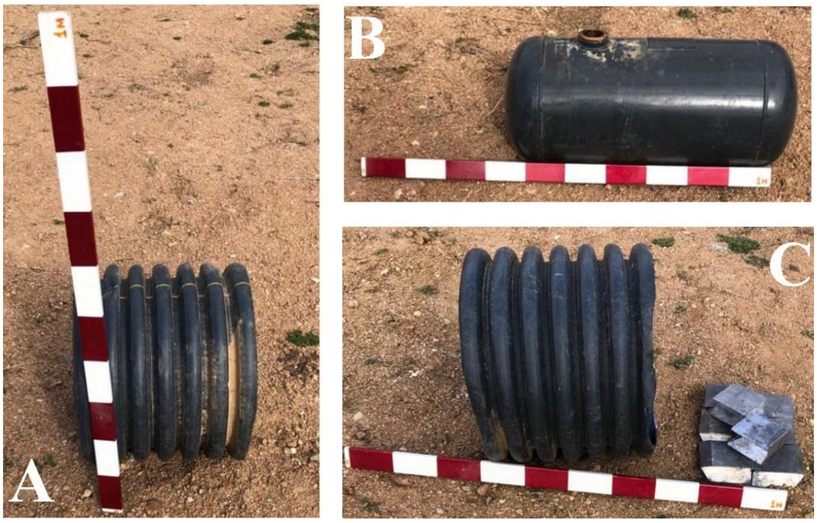

Figure 3. Objects with different material properties to be buried in the test site

The test site was first limited with white lime, with a width of 80 cm and a length of 5 m, and excavation began with the help of ladle (CAT brand) at a depth of 5 m. (Figure 4). After the excavation process was completed, buried objects A, B and C began to be placed at a certain depth in the excavated area (Figure 5). The intermediate layer was filled with truck-transported sand before being once again covered with soil filling. The test area covered with the filling material was made ready for the GPR measurement by limiting it with white lines as was done at the beginning.

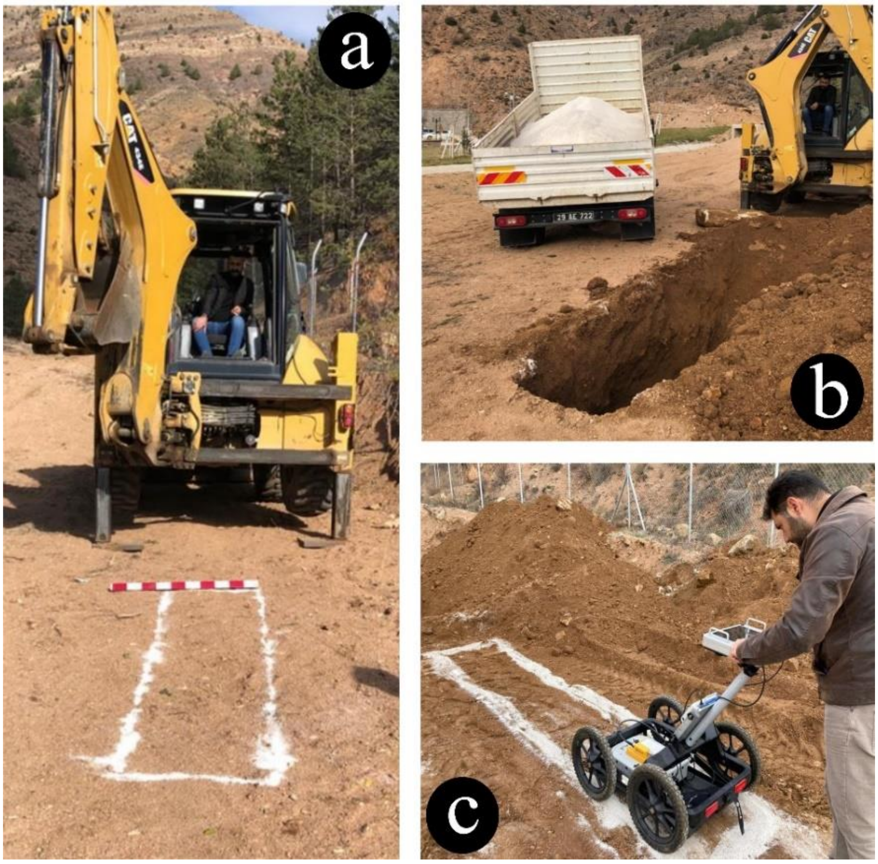

Figure 4. a) Excavation of the limited test area with the help of ladle, b) pouring sand into the interlayer with a truck, c) reaching the measurement stage of the filled test area with GPR

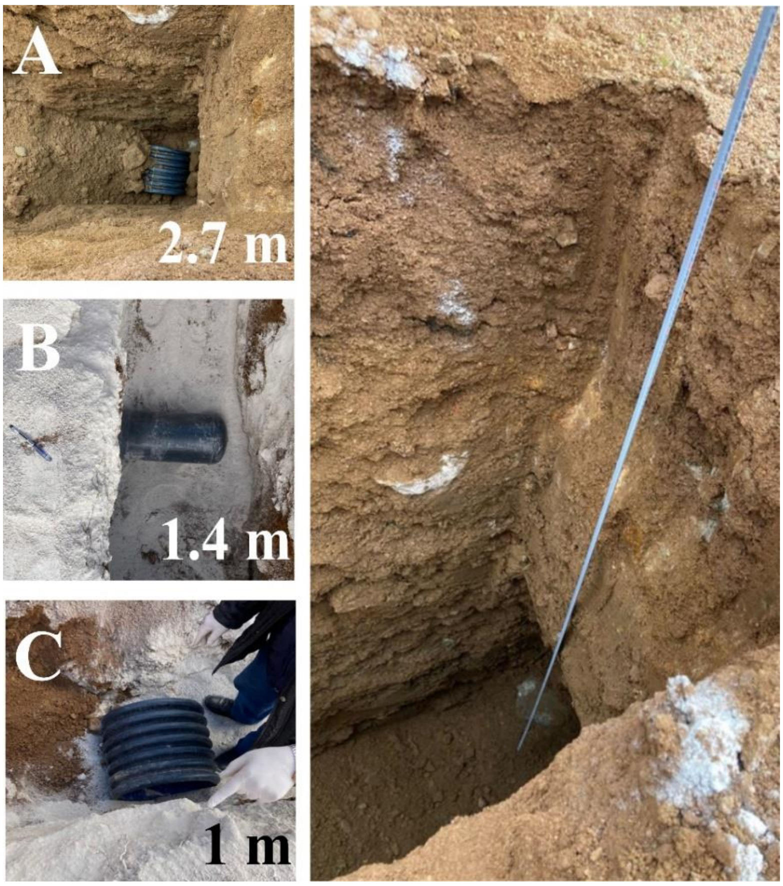

Figure 5. Depths where buried objects with different material properties are placed

GPR measurements were taken in 1 profile (5m long) in a way that cuts the buried objects vertically in the limited test area. The parameters used in GPR measurements are given in Table 2. Data processing steps applied to the obtained GPR raw data are given in Table 3.

Table 2. GPR measurement parameters used during field studies

Measurement parameters	
Antenna freq	500 MHz
Trace interval	1 cm
Samples	512
Sampling freq.	5862 MHz
Time window	60.24 ns
Profile intervals	50 cm

Table 3. Filter processing steps and parameters of the GPR data

Filter name	Parameters
Time-zero correction	-4.5 ns
Subtract-mean (dewow)	2 ns
Energy decay	0.512
Subtracting average	31 trace – 0 to 60.24 ns
Band-pass filter	200-400-600-800 MHz
Velocity analysis	0.1 m ns^{-1}
Diffraction stack migration	31 trace/ 0.1 m ns^{-1}/0-60.24 ns

4. Results and discussion

The working test area was determined to be 5m in length, 5m in depth and 80 cm in width, and ground radar measurements were started by burying objects selected from plastic and iron materials (Figure 6). The two-dimensional ground radar section of the ground radar method reveals the position, size, amplitude, hyperbola, and scattering states of the buried items (Figure 7).

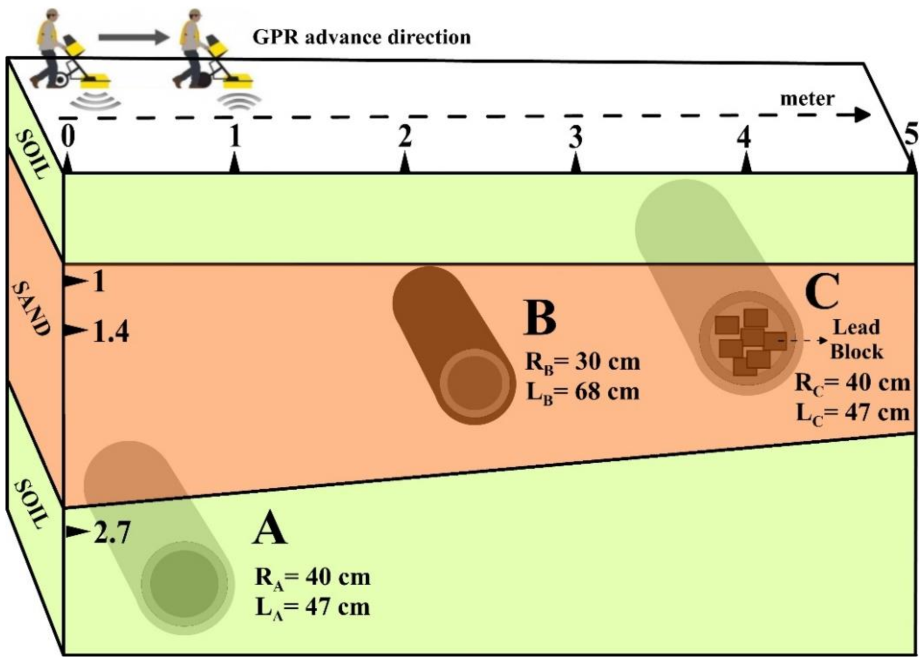

Figure 6. Subterranean states of buried objects with different material properties

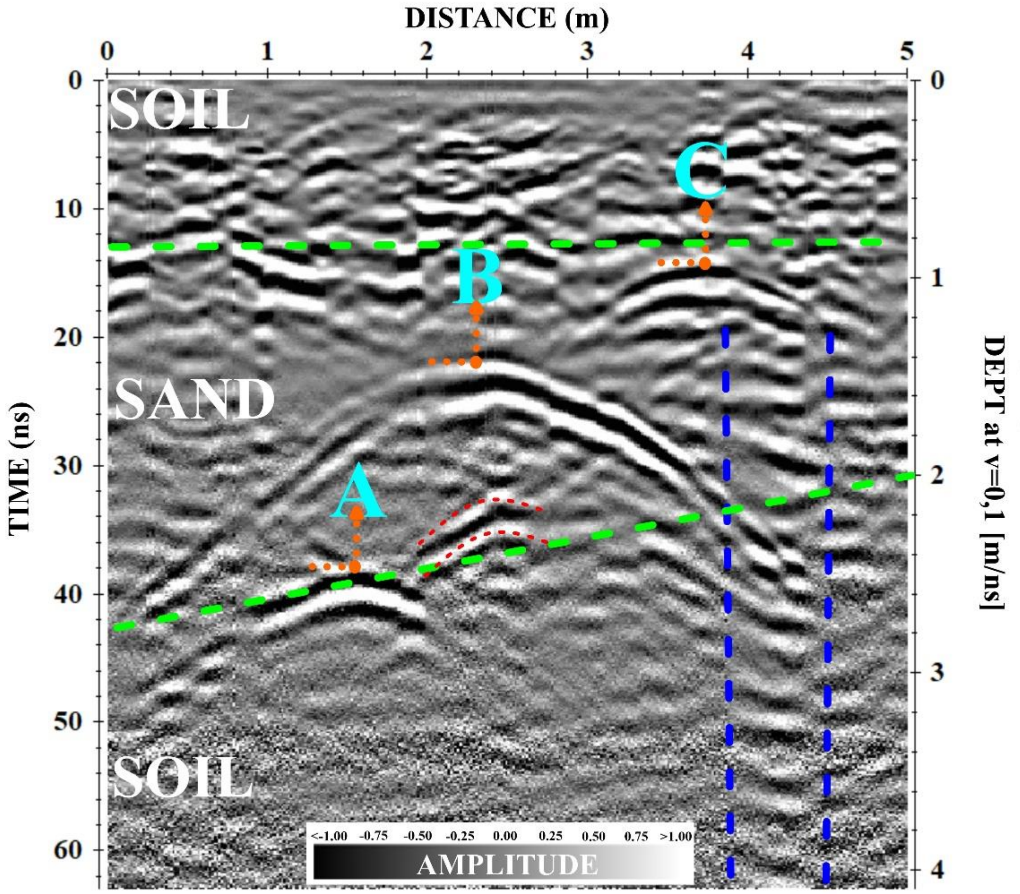

Figure 7. Two-dimensional radar cross section of buried objects with different material properties

The positions of the objects with various material properties buried underneath were clearly shown by the GPR measurement findings obtained in the research region. Hyperbola peaks of buried objects are marked with an orange circle and marked A, B, and C on the figure. A hyperbola peak is 2.7m, B hyperbola peak is 1.4 and C hyperbola peak is 1m in radargram sections and it has been determined that they are exactly the same as the measurements in their buried state. Since the filling materials of the two-dimensional radar cross-section are known, the depth information and layer conditions determined by the simple "depth=velocity x time / 2" approach can be determined by using the velocity and time information. In Figure 7, the upper green line indicates the upper soil boundary, and the sand material boundary between the two green lines. Since the sand area is homogeneous, it gives us a clearer image on the radargram. It is seen that the reflections of the lead blocks we put in the plastic pipe in the C hyperbola peak region continue to the lowest depth (The region indicated by the blue dashed line in Figure 7). The amplitude and polarity of the reflected/scattered wave fields are effective in determining the type of pipe (Kurt et al., 2009). The EM wave velocities of the metals iron and plastic, which we utilize as buried objects in this work, are known to be 0.017 m/ns and 0.16 m/ns, respectively (Zeng & McMechan, 1997). Accordingly, under normal conditions, the scattered wave fields from the iron pipe are of negative polarity and the wave fields from the very high amplitude plastic pipe are of positive polarity and low amplitude. Also, due to the high amplitude, repeated scattered wave field hyperbolas can be seen inside the hollow large diameter pipe (Shown with red lines in Figure 7). Additionally, the dry EM wave velocities of sandy soil and sand are 0.13 m/ns and 0.19 m/ns, respectively (Leckebusch, 2003). Dry sand and plastic pipes EM wave velocities being relatively close to one another, the reflection coefficient value of the plastic pipe is lower than that of the iron pipe. Therefore, the scattered wave field hyperbolas of the plastic pipe attenuate faster than the scattered wave field hyperbolas of the smaller diameter iron pipe (In Figure 7, A and C are damped faster than B amplitude). Also, absent from the scattering hyperbolas of the plastic pipe are in-pipe repetitions (ringing) (Figure 7).

5. Conclusions

In the study, it is carried out to detect buried objects with different material properties by ground radar method. The results obtained by examining the GPR measurement are given below.

- The positions of buried objects with different material properties are clearly identified.
- It is known that the amplitudes of the scattered wave fields coming from the iron pipe are significantly larger than those coming from the plastic pipe.
- It has been discovered that the magnitudes of the amplitudes depend on the EM wave field velocities of the medium and pipes as well as the associated reflection coefficients.
- The scattered wave field hyperbolas of the plastic pipe have been shown to attenuate more quickly than those of the smaller diameter iron pipe. It has been determined that intra-pipe repetitions (ringing) are not seen in the scattering hyperbolas of the plastic pipe, but only in the iron pipe.

Acknowledgement

I would like to thank Gümüşhane University for making us use the construction machines during my field work, Ustaoğlu Group Ready-Mixed Concrete for providing us with the necessary sand transport, and Dr. Ersin BÜYÜK for their contributions during the measurement.

Author contribution

The manuscript was written by the corresponding author.

Declaration of ethical code

The author declares that the materials and methods used in this study do not require ethical committee approval or legal-specific permission.

Conflict of interest

The authors declare no conflict of interest.

References

Annan, A. (2005). Ground-penetrating radar. In *Near-surface geophysics* (pp. 357-438). Society of Exploration Geophysicists.

Annan, A., & Davis, J. (1977). Impulse radar applied to ice thickness measurements and freshwater bathymetry. *Geological Survey of Canada, Report of Activities Paper*, *77*, 117-124.

Aydın, Z. O., Babacan, A. E., Seren, A., & Gelisli, K. (2022). New historical findings discovery at inner areas of Akçakale Castle (Trabzon, Turkey) with GPR Method. *Sigma Journal of Engineering and Natural Sciences*, *40*(2), 344-355.

Carcione, J. M., Seriani, G., & Gei, D. (2003). Acoustic and electromagnetic properties of soils saturated with salt water and NAPL. *Journal of Applied Geophysics*, *52*(4), 177-191. https://doi.org/10.1016/S0926-9851(03)00012-0.

Daniels, D. J. (2004*). Ground penetrating radar* (Vol. 2nd edition). The Institution of Electrical Engineers.

Davis, J., & Annan, A. (1986). Machinations: high-resolution sounding using ground-probing radar. *Geoscience Canada*.

Davis, J. L., & Annan, A. P. (1989). Ground-penetrating radar for high-resolution mapping of soil and rock stratigraphy 1. *Geophysical prospecting*, *37*(5), 531-551.

Hammon III, W. S., McMechan, G. A., & Zeng, X. (2000). Forensic GPR: finite-difference simulations of responses from buried human remains. *Journal of Applied Geophysics*, *45*(3), 171-186. https://doi.org/10.1016/S0926-9851(00)00027-6.

Hugenschmidt, J. (2002). Concrete bridge inspection with a mobile GPR system. *Construction and building materials*, *16*(3), 147-154.

Kurt, B., Kadıoğlu, S., & Ekincioğlu, E. (2009). Determination of the location, size and physical characteristics of buried pipes by ground penetrating radar method Yer radarı yöntemi ile gömülü boruların konum, büyüklük ve fiziksel özellikleri ile belirlenmesi. *Yerbilimleri/Earth Sciences*, *30*(1).

Kurtulmuş, T. Ö., & Drahor, M. G. (2008). Yer radarı modellemesinde fiziksel ve geometrik parametre etkilerinin araştırılması. *Yerbilimleri*, *29*(2), 37-52.

Leckebusch, J. (2003). Ground-penetrating radar: a modern three-dimensional prospection method. *Archaeological prospection*, *10*(4), 213-240.

Lopera, O., Milisavljević, N., & Lambot, S. (2007). Clutter reduction in GPR measurements for detecting shallow buried landmines: a Colombian case study. *Near Surface Geophysics*, *5*(1), 57-64. https://doi.org/10.3997/1873-0604.2006018.

Neubauer, W., Eder-Hinterleitner, A., Seren, S., & Melichar, P. (2002). Georadar in the Roman civil town Carnuntum, Austria: an approach for archaeological interpretation of GPR data. *Archaeological prospection*, *9*(3), 135-156. https://doi.org/10.1002/arp.183.

Ramac/GPR. (n.d). Operating manual version 1. https://fcc.report/FCC-ID/QLASH1GHZ/375215.pdf

Sari, M., & Öztürk, S. (2018). Detection of the complex ground problems by ground penetrating radar: Examples from Gümüşhane University. *Sigma Journal of Engineering and Natural Sciences*, *36*(4), 1297-1310.

Sarıçiçek, I., & Şeren, A. (2020). In-Sıtu Wall Concrete Qualıty Usıng Velocıty Fıeld-Dependent Mıgratıon In Zıgana And Torul Tunnels. *Sigma Journal of Engineering and Natural Sciences*, *38*(2), 979-993.

Streich, R., Van der Kruk, J., & Green, A. G. (2006). Three-dimensional multicomponent georadar imaging of sedimentary structures. *Near Surface Geophysics*, *4*(1), 39-48. https://doi.org/10.3997/1873-0604.2005030.

ULiege & BGS. (n.d). Introduction to Ground Penetrating Radar. https://vb.nweurope.eu/media/12924/5-rawfill-training-days_geophysics_gpr.pdf

Uyar, Ş. (2017*). Investigation of problems in clean and waste water infrastructure systems with georadar method*. KTU Institute of Science.

Zeng, X., & McMechan, G. A. (1997). GPR characterization of buried tanks and pipes. *Geophysics*, *62*(3), 797-806. https://doi.org/10.1190/1.1444189.